IEEE Access
Multidisciplinary | Rapid Review | Open Access Journal

Received 6 January 2023, accepted 14 January 2023, date of publication 20 January 2023, date of current version 25 January 2023.

*Digital Object Identifier 10.1109/ACCESS.2023.3238663*

RESEARCH ARTICLE

# Influence of Dynamic Accuracy Constraints of Manipulator of Wafer Transmission Robot on Scheduling and Control of Single-Armed Cluster Tools

**TINGHAO LI[1,2] AND ZHANGUANG ZHENG[3]**

[1]Institute of Systems Engineering, Macau University of Science and Technology, Macau 999078, China
[2]Collaborative Laboratory for Intelligent Science and Systems, Macau University of Science and Technology, Macau 999078, China
[3]College of Mechanical Engineering, Guangxi University, Nanning 530004, China

Corresponding author: Zhanguang Zheng (zhenglight@126.com)

This work was supported in part by the National Natural Science Foundation of China under Grant 52265018.

**ABSTRACT** The wafer transfer robot is a key part of integrated circuit equipment which performs the transit of wafers precisely, quickly and steadily. The dynamic accuracy of the manipulator of the wafer transfer robot directly affects the quality of transferring and processing wafers and even the scheduling and control of the cluster tools. Thus, it is essential to study the influence of the dynamic accuracy of the manipulator of wafer transmission robots on the scheduling and control of cluster tools. In this paper, single-arm cluster tools are taken as the research object. The horizontal torsional vibration equations of the manipulator of the $R$-$\theta$ robot are constructed, and the torsional vibration attenuation characteristics of the manipulator are analyzed. Based on the torsional vibration equations, the intrinsic relationships between the dynamic accuracy of the manipulator and the waiting times of the manipulator are explored when the manipulator loads and unloads the wafers. Then the two-stage approach is proposed for the scheduling and control of single-arm cluster tools. The first stage determines the minimum waiting times of the manipulator according to the intrinsic relationships between the dynamic accuracy of the manipulator and the waiting times of the manipulator when the manipulator is waiting for loading and unloading wafers in each processing module and load lock. The second stage achieves the scheduling optimization and control of single-arm cluster tools with dynamic accuracy constraints and wafer residency time constraints by establishing a mathematical programming model for the scheduling and control of single-arm cluster tools. Finally, illustrative examples are presented to analyze the influence of the dynamic accuracy of the manipulator on the scheduling and control of single-arm cluster tools.

**INDEX TERMS** Wafer fabrication, single-arm cluster tools, manipulator, dynamic accuracy, residency time, scheduling.

## I. NOMENCLATURE

| *Symbol* | *Annotations* |
|---|---|
| $n$ | Number of wafer fabrication processes. |
| $PM_i$ | The $i$-th processing module in the single-arm cluster tools, $\{i \in 1, 2, \cdots, n\}$. |
| $PM_0$ | Load lock in the single-arm cluster tools. |
| $s_{i1}$ | Load wafers into $PM_i$, $\{i \in 0, 1, 2, \cdots, n\}$. |
| $s_{i2}$ | Unload wafers from $PM_i$ and move to $PM_{i+1}$, $\{i \in 0, 1, 2, \cdots, n\}$. |
| $s_{n2}$ | Unload wafers from $PM_n$ and move to load lock. |
| $y_i$ | Move from $PM_{i+2}$ to $PM_i$ with no load, $\{i \in 0, 1, 2, \cdots, n-2\}$. |
| $y_{n-1}$ | Move from load lock to $PM_{n-1}$. |
| $y_n$ | Move from $PM_1$ to $PM_n$. |
| $p_i$ | Wafers are processed in $PM_i$, $\{i \in 0, 1, 2, \cdots, n\}$. |
| $q_{i1}$ | Wait to load wafer into $PM_i$, $\{i \in 0, 1, 2, \cdots, n\}$. |

The associate editor coordinating the review of this manuscript and approving it for publication was Kuo-Ching Ying.

| | |
|---|---|
| $q_{i2}$ | Wait to unload wafer from $PM_i$, $\{i \in 0, 1, 2, \cdots, n\}$. |
| $r$ | Status of the manipulator. |
| $m_i$ | Number of parallel PM for the $i$-th process. |
| $M$ | Identification of the number of tokens in the place in the Petri net. |
| $M_0$ | Initial identification of the number of tokens in the place in the Petri net. |
| $T_Z$ | Time required for the manipulator to run in steady state for a cycle. |
| $T_{Z1}$ | Total action time of the manipulator in a steady operation cycle. |
| $T_{Z2}$ | Total waiting time of the manipulator in a steady operation cycle. |
| $T_{Li}$ | Lower bound of production cycle for the completion of the $i$-th process by the single-arm cluster tools, $\{i \in 1, 2, \cdots, n\}$. |
| $T_{Li\min}$ | Minimum value of lower bound of production cycle for the completion of the $i$-th process by the single-arm cluster tools, $\{i \in 1, 2, \cdots, n\}$. |
| $T_{Si1}$ | Time to load wafer into $PM_i$ or load lock by the manipulator, $\{i \in i \in 0, 1, 2, \cdots, n\}$. |
| $T_{Si2}$ | Time to unload wafer from $PM_i$ or load lock by the manipulator, $\{i \in 0, 1, 2, \cdots, n\}$. |
| $T_{Mij}$ | Time for the manipulator to move from $PM_i$ to $PM_j$, $i, j \in 0, 1, 2, \cdots, n$. |
| $T_{C0}$ | Time for the manipulator to unload wafer from the load lock and perform alignmen. |
| $T_P$ | System cycle under steady schedule of the single-arm cluster tools. |
| $T_{PF}$ | Optimal system cycle under steady schedule of the single-arm cluster tools. |
| $T_{Pi}$ | Actual residency time of the wafer during being processed in $PM_i$, $\{i \in 1, 2, \cdots, n\}$. |
| $T_{Pi\min}$ | Minimum residency time required for processing wafers in $PM_i$, $\{i \in 1, 2, \cdots, n\}$. |
| $T_{Pi\max}$ | Maximum residency time required for processing wafer in $PM_i$, $\{i \in 1, 2, \cdots, n\}$. |
| $T_{Wi1}$ | Waiting time to load wafer into $PM_i$ or load lock, $\{i \in 0, 1, 2, \cdots, n\}$. |
| $T_{Wi2}$ | Waiting time to unload wafer from $PM_i$ or load lock, $\{i \in 0, 1, 2, \cdots, n\}$. |
| $T_{Wi1\min}$ | Minimum waiting time for the manipulator to wait to load wafer into $PM_i$ or load lock, $\{i \in 0, 1, 2, \cdots, n\}$. |
| $T_{Wi2\min}$ | Minimum waiting time for the manipulator to wait to unload wafer from $PM_i$ or load lock, $\{i \in 0, 1, 2, \cdots, n\}$. |
| $T_{Wi\max}$ | Maximum value of the sum of the waiting time of the manipulator in the $i$-th process, $\{i \in 1, 2, \cdots, n\}$. |

## II. INTRODUCTION

In single-arm cluster tools, the wafer transfer robot is mainly responsible for transferring and positioning wafers between multiple stations [1], [2]. When the wafer transfer robot rapidly transfers the wafers from one workstation to another workstation within the limited working space and operating time, the dynamic accuracy of the wafer transfer robot directly affects the quality of transferring and processing wafers and even the reliability of the entire semiconductor fabrication system [3], [4]. The wafer transfer robot goes through the process from the steady state to the braking state when it loads and unloads the wafers, and the change in operation states will result in inertial forces that are exerted on the wafer transfer robot. Under the effect of inertial forces, forced vibration will take place in the wafer transfer robot, which affects the dynamic accuracy of the wafer transfer robot. Therefore, the objective of this paper is to elucidate the scheduling and control of single-armed cluster tools with dynamic accuracy constraint and wafer residency time constraint.

### A. RESEARCH MOTIVATION

The vibration of the wafer transfer robot often results in a decrease in the dynamic accuracy of the wafer transfer robot, which in turn directly affects the quality of transferring and processing wafers. Therefore, it is necessary to consider the dynamic accuracy constraints of the wafer transfer robot when the single-arm cluster tools are better scheduled and controlled. Therefore, the research motivations behind this work are listed as follows:

1) Make the scheduling model of cluster tools more accurately reflect the actual situation by taking into account the influence of the dynamic accuracy constraints of the manipulator of wafer transmission robot.

2) Ensure the processing quality of wafers to satisfy the production requirements and reduce the reject rate of wafers.

3) Increase the productivity of cluster tools by improving the wafer residency time delays.

4) Propose the approach for the scheduling and control of single-arm cluster tools with dynamic accuracy constraints and wafer residency time constraints.

### B. PREVIOUS SURVEYS

#### 1) DYNAMIC CHARECTERISTICS OF ROBOT MANIPULATOR

As the requirements for the dynamic performance of wafer transfer robots have increased, increasing attention has been given to the vibration characteristics of wafer transfer robots. For example, Duong and Terashima [5] propose a vibration suppression tool with visual graphical interface to solve the vibration problem based on input shaping approach, and applies the proposed tool in real industry processes to solve the vibration problems of semiconductor wafer transfer robot. Wang et al. [6] introduce an active wide-band vibration rejection method with a vibrotactile actuator and applies it to a wafer transfer robot, and experimental validation shows a vibration reduction of more than 40% in energy and 30% in amplitude. Aribowo et al. [7] present an integrated tool of parameter identification and vibration control for higher modes vibration systems, as an easy and effective tool to help industrial people to analyze and solve the vibration problem.

Liu et al. [8] establish the wafer transfer robot dynamic model and proposes the strategy of vibration suppression based on input shaping, so as to solve the vibration during the process of transferring wafers and achieve the purpose of transferring wafers accurately and stably. However, in many industrial applications, flexible joints and links have a significant effect on the accuracy of the desired trajectory of the end effector. Therefore, some scholars have studied the influence of flexible joints and links on the dynamic characteristics of robot manipulators. For example, Korayem et al. investigate the effects of joint flexibility on optimizing the dynamic loadcarrying capacity the maximum payload value [9], [10], and present a general formulation for finding the maximum allowable dynamic load of flexible link mobile manipulators [11]. Ma et al. propose an adaptive fuzzy control strategy for a single-link flexible-joint robotic manipulator with prescribed performance [12].

#### 2) SCHEDULING ANALYSIS AND OPTIMIZING OF CLUSTER TOOLS

Cluster tools are highly automated and integrated equipment that are broadly applied in wafer fabrication processes [13], [14]. To effectively improve the production efficiency and yield rate of wafers, many scholars have extensively investigated these problems regarding the scheduling and control of single-armed cluster tools with different constraints. For example, since the batches have different operating costs and consecutive steps of a job are constrained with time links, Kim et al. [15] present a hybrid two-stage solution strategy, combining Mixed Integer Linear Programming (MILP) models and heuristics and minimizes the total weighted batching cost, queuing time, and the number of violations of time link constraints. May et al. [16] present a data-based decision process to predict time constraint adherence in semiconductor manufacturing, analyzes the real-world historical data, and derives the appropriate statistical models and scoring functions, and so on.

However, for some wafer fabrication processes, such as low pressure chemical-vapor deposition (LPCVD), the wafer residency time constraints cannot be ignored [17], [18]. This means that the wafer residency times in the processing modules (PMs) must be within the limited ranges. Otherwise, the wafers may be damaged by residual gases or residual temperature inside the PMs. In addition, the scheduling and control of cluster tools with wafer residency time constraints are often complicated since there is no buffer set in the system. Therefore, many scholars have intensively studied the scheduling and control of cluster tools with wafer residency time constraints. For example, Qiao et al. [19] propose a novel virtual wafer-based scheduling method to provide a solution for dual-arm cluster tools with strictly wafer residency time constraints and chamber cleaning requirements. Lim et al. [20] examine a scheduling problem for cluster tools with strict upper limits on wafer delays under process time variation and proposes a new class of schedules, which not only keeps timing patterns steady as possible but also adapts timing of tasks in response to process time variation so as to satisfy wafer delay constraints robustly.

According to the structure of the robot, the cluster tools are divided into two-arm cluster tools and single-arm cluster tools. The methods of scheduling and control are also quite different for different types of cluster tools. Therefore, the problems of scheduling and control of two-arm cluster tools and single-arm cluster tools with wafer residency time constraints have been studied. For example, in order to meet the wafer residency time constraints, Qiao et al. [21] propose PM failure response policies which can successfully transfer a cluster tools to the feasible schedule after failure from the one before a failure, and develops efficient algorithms to improve these response policies which are composed of simple control laws. Wang et al. [22] investigate the scheduling problems of dual-arm cluster tools with multiple wafer types and residency time constraints, and develops a novel robot activity strategy called multiplex swap sequence so as to pursue an easy-to-implement cyclic operation under diverse flow patterns. Yang et al. [23] study the challenging problem for scheduling a single-arm cluster tool with wafer residency time constraints and uses a timed Petri net to model the dynamic behavior of the system and presents a method to determine the optimal scheduling strategy for the system, and reveals that the key issue to schedule such a tool is to determine when and how long the robot should wait for. Pan et al. [24] are devoted to regulating the robot waiting times in single-arm cluster tools under steady state such that the wafer residency time delay can be offset as much as possible, and presents a priority rule for assigning robot waiting times.

### C. CONTRIBUTIONS

At present, although many achievements have been made in the research of real-time scheduling and control of cluster tools, the influence of the dynamic accuracy on scheduling and control of cluster tools has not been considered in these studies. The contributions of our research can be summarized as follows:

1) We construct the horizontal torsional vibration equations of the manipulator of $R$-$\theta$ robot and reveal the horizontal torsional vibration attenuation characteristics of the manipulator.

2) We derive the calculation formula of the dynamic accuracy of the manipulator when loading and unloading wafers, and discover the intrinsic relationship between the dynamic accuracy of the manipulator and the waiting time required when loading and unloading wafers.

3) We establish the mathematical programming model for scheduling and control of single-arm cluster tools with dynamic accuracy constraints and wafer residency time constraints based on the two-stage approach.

4) We propose the method for achieving the scheduling optimization and control of single-arm cluster tools with dynamic accuracy constraints and wafer residency time constraints.

### D. STRUCTURE OF THIS PAPER

This paper has been organized in such a way that the background information for the research comes first. The remainder of this paper is organized as follows. Section III establishes the torsional vibration equations of the manipulator of the $R$-$\theta$ robot and then reveals the intrinsic relationships between the dynamic accuracy of the manipulator and the waiting times of the manipulator. Section IV proposes a two-stage approach for the scheduling and control of single-arm cluster tools. Section V presents illustrative examples to show the application of the proposed method. Finally, Section VI gives the conclusions.

## III. DYNAMIC ACCURACY OF MANIPULATOR OF ROBOT

### A. VIBRATION DIFFERENTIAL EQUATION

The wafer transfer robot is responsible for transferring the wafers between the various workstations. The main structural forms of common transfer robots are divided into two types [25]: SCARA type (planar joint type) and $R$-$\theta$ type (polar coordinate type). The SCARA wafer transfer robot controls one degree of freedom per joint, and the motion is flexible and simple. However, there is nonlinear coupling between each degree of freedom, which is not convenient to control. In contrast, the $R$-$\theta$ wafer transfer robot easily performs the inverse solution of dynamics, although the structure form and transmission principle are more complicated. This type of robot is widely used because it is easy to control in applications. Thus, the scheduling and control of single-arm cluster tools with the $R$-$\theta$ wafer transfer robot is considered here, as shown in Figure 1.

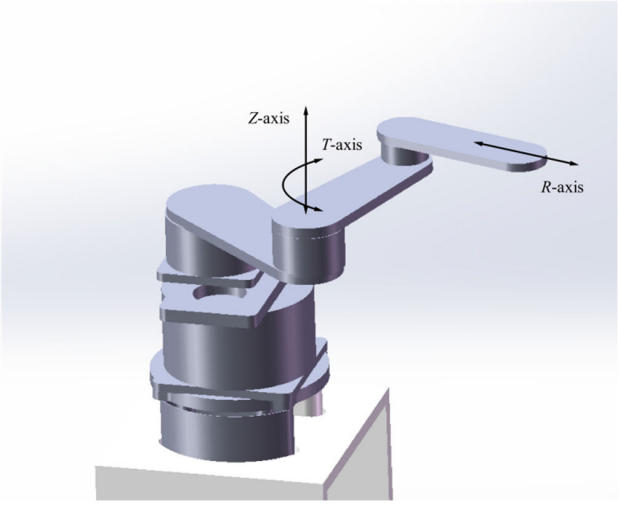


**FIGURE 1.** R-$\theta$ wafer transfer robot.

The $R$-$\theta$ wafer transfer robot is based on the structure of column coordinates, and the line between any point in space and the origin of the wafer transfer robot forms a vector. The $Z$-directional component of the vector is the $Z$-axis of the wafer transfer robot, and the $Z$-axis coordinate reflects the displacement of the wafer transfer robot along the vertical direction. The component of the vector in the horizontal plane is expressed by polar coordinates, the $R$-axis coordinate represents the kinematics displacement in polar coordinates, and the $T$-axis coordinate represents the angular displacement in polar coordinates.

When the $R$-$\theta$ wafer transfer robot loads and unloads wafers, the processes are as follows [26]: First, the $R$-axis is stationary, and the $T$-axis and $Z$-axis move simultaneously so that the robot can reach a position with a certain height and angle so that the end-effector of the manipulator of the robot can reach into the CST and maintain a certain height with the wafer. Then, the $Z$-axis is stationary, while the $T$-axis moves in coordination with the $R$-axis, and the end-effector of the manipulator reaches inside the CST where it waits and remains static. Finally, the wafers are loaded and unloaded by the end-effector of the manipulator.

According to elastic dynamics theory, inertial forces are generated when the end-effector of the manipulator of the $R$-$\theta$ wafer transfer robot reaches inside the CST and remains static. Under the action of inertial forces, forced vibration will take place in the manipulator, which affects the dynamic accuracy of the manipulator during loading and unloading wafers. To effectively control the dynamic accuracy of the end-effector of the manipulator, it is necessary to analyze the elastic dynamics characteristics of the end-effector of the manipulator when it reaches inside the CST and remains static and to explore the vibration attenuation mechanism of the end-effector of the manipulator to realize the effective scheduling and control of the single-arm cluster tools.

The T-axis and R-axis of the R-$\theta$ wafer transfer robot are driven by the harmonic drive, and the R-axis in turn drives the rotation of the large and small arms and the telescopic movement of the end-effector of the manipulator of the robot by the synchronous belts. When the end-effector of the manipulator reaches inside the CST and remains static, torsional vibration will take place in the manipulator around the flexible joint in the horizontal direction under the action of the inertial force in the horizontal direction. Therefore, the torsional vibration characteristics of the manipulator are analyzed and studied when the end-effector of the manipulator reaches inside the CST and remains static. Because there are many flexible elements inside each arm joint of the manipulator, the joints of the manipulator of the R-$\theta$ wafer transfer robot joints can be considered flexible joints. Since the synchronous belts of the manipulator are very flexible, the flexibility of the synchronous belts can be equivalent to that of the joints. Thus, here, the flexible joints (including the synchronous belts) are equivalent to the linear torsional elastic elements. If each arm of the manipulator is considered as a rigid rod, the mechanical model of the torsional vibration system of the manipulator is shown in Figure 2.

In Figure 2, rods OA, AB, BC are the big arm, small arm and end arm of the manipulator, respectively; $l_1, l_2, l_3$ are the lengths of rods OA, AB and BC, respectively; $O_1, O_2, O_3$ are the centroids of rods OA, AB and BC, respectively, and the lengths of $O_1O$, $O_2A$, $O_3B$ are denoted as $l_{O1}$, $l_{O2}$ and $l_{O3}$,

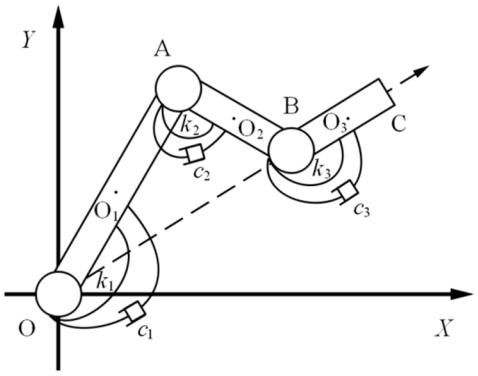


**FIGURE 2.** Mechanical model of the torsional vibration system of manipulator.

respectively; $k_1$, $k_2$, $k_3$ are the equivalent torsional stiffness coefficients at joints O, A, and B, respectively; $c_1$, $c_2$, $c_3$ are the equivalent torsional damping coefficients at joints O, A, and B, respectively.

According to the operating principle of the $R$-$\theta$ wafer transfer robot [26], it is known that

$$l_1 = l_2 \tag{1}$$

$$(\theta_1 - \theta_3) : (\theta_1 - \theta_2) : (\theta_3 - \theta_2) = 1 : 2 : 1 \tag{2}$$

where $\theta_1$, $\theta_2$ and $\theta_3$ are the angle between rod OA and $X$-axis, the angle between the rod AB and $X$-axis, and the angle between rod BC and $X$-axis, respectively.

Obviously, $\theta_1$, $\theta_2$ and $\theta_3$ are also the absolute motion angular displacements of rods OA, AB and BC, respectively. According to the knowledge of elastic dynamics, the absolute motion angular displacements can be expressed as

$$\theta_1 = \theta_{r1} + \tilde{\theta}_1 \tag{3}$$

$$\theta_2 = \theta_{r2} + \tilde{\theta}_2 \tag{4}$$

$$\theta_3 = \theta_{r3} + \tilde{\theta}_3 \tag{5}$$

where $\theta_{r1}$, $\theta_{r2}$, $\theta_{r3}$ are the rigid body motion angular displacements of rods OA, AB and BC; $\tilde{\theta}_1$, $\tilde{\theta}_2$, $\tilde{\theta}_3$ are the elastic motion angular displacements of rods OA, AB, BC.

Since the total kinetic energy $T$ of the torsional vibration system is the sum of the kinetic energy of the rods OA, AB and BC, the total kinetic energy $T$ can be written as

$$T = \frac{1}{2}\dot{\boldsymbol{\theta}}^{\mathrm{T}} M \dot{\boldsymbol{\theta}} \tag{6}$$

where $\boldsymbol{M}$ is the mass matrix of the torsional vibration system, $\dot{\boldsymbol{\theta}}$ is the absolute angular velocity vector of the torsional vibration system, and

$$\boldsymbol{M} = \begin{bmatrix} m_{11} & m_{12} & 0 \\ m_{21} & m_{22} & 0 \\ 0 & 0 & m_{33} \end{bmatrix}, \dot{\boldsymbol{\theta}} = \begin{Bmatrix} \dot{\theta}_1 \\ \dot{\theta}_2 \\ \dot{\theta}_3 \end{Bmatrix}$$

$$m_{11} = J_{O1} + m_1 l_{O1}^2 + m_2 l_1^2$$

$$m_{22} = J_{O2} + m_2 l_{O2}^2$$

$$m_{33} = J_{O3} + m_3[2l_1 \cos(\theta_1 - \theta_3) + l_{O3}$$

$$m_{12} = m_{21} = -m_2 l_1 l_{O2} \cos(\theta_1 - \theta_2)$$

where $J_{O1}$ is the equivalent moment of inertia of rod OA with respect to its centroid $O_1$; $J_{O2}$ is the equivalent moment of inertia of rod AB with respect to its centroid $O_2$; $J_{O3}$ is the equivalent moment of inertia of rod BC with respect to its centroid $O_3$; $\dot{\theta}_1$, $\dot{\theta}_2$, $\dot{\theta}_3$ are the absolute angular velocities of rods OA, AB and BC, respectively; $m_1$, $m_2$, $m_3$ are the equivalent mass of rods OA, AB and BC, respectively.

Since the total elastic potential energy of the torsional vibration system is the sum of the elastic potential energy of the equivalent torsional elastic elements at joints O, A and B, the total elastic potential energy $N$ of the torsional vibration system can be expressed as

$$N = \frac{1}{2}\tilde{\boldsymbol{\theta}}^{\mathrm{T}} K \tilde{\boldsymbol{\theta}} \tag{7}$$

where $\boldsymbol{K}$ is the stiffness matrix of the torsional vibration system, $\tilde{\theta}$ is the elastic angular displacement vector of the torsional vibration system, and

$$\boldsymbol{K} = \begin{bmatrix} k_1 + k_2 & -k_2 & 0 \\ -k_2 & k_2 + k_3 & -k_3 \\ 0 & -k_3 & k_3 \end{bmatrix}, \tilde{\boldsymbol{\theta}} = \begin{Bmatrix} \tilde{\theta}_1 \\ \tilde{\theta}_2 \\ \tilde{\theta}_3 \end{Bmatrix}$$

Since the total dissipated energy of the torsional vibration system is the sum of the dissipated energy of the equivalent damping elements at joints O, A and B, the total dissipated energy $D$ of the torsional vibration system can be expressed as

$$D = \frac{1}{2}\dot{\tilde{\boldsymbol{\theta}}}^{\mathrm{T}} C \dot{\tilde{\boldsymbol{\theta}}} \tag{8}$$

where $\boldsymbol{C}$ is the damping matrix of the torsional vibration system of the robot, $\dot{\tilde{\theta}}$ is the elastic angular velocity vector of the torsional vibration system, and

$$\boldsymbol{C} = \begin{bmatrix} c_1 + c_2 & -c_2 & 0 \\ -c_2 & c_2 + c_3 & -c_3 \\ 0 & -c_3 & c_3 \end{bmatrix}, \dot{\tilde{\boldsymbol{\theta}}} = \begin{Bmatrix} \dot{\tilde{\theta}}_1 \\ \dot{\tilde{\theta}}_2 \\ \dot{\tilde{\theta}}_3 \end{Bmatrix}$$

where $\dot{\tilde{\theta}}_1$, $\dot{\tilde{\theta}}_2$ and $\dot{\tilde{\theta}}_3$ are the elastic angular velocities of rods OA, AB and BC, respectively.

Lagrange equation which is used in the torsional vibration system can be expressed as

$$\frac{\mathrm{d}}{\mathrm{d}t}\frac{\partial T}{\partial \dot{\tilde{\theta}}_i} - \frac{\partial T}{\partial \tilde{\theta}_i} + \frac{\partial V}{\partial \tilde{\theta}_i} + \frac{\partial D}{\partial \dot{\tilde{\theta}}_i} = F_i \quad (i = 1,\ 2,\ 3) \tag{9}$$

Substituting (6), (7) and (8) into (9), rearranging, the torsional vibration equation of the torsional vibration system is obtained as

$$\boldsymbol{M}\ddot{\tilde{\boldsymbol{\theta}}} + \boldsymbol{C}\dot{\tilde{\boldsymbol{\theta}}} + \boldsymbol{K}\tilde{\boldsymbol{\theta}} = \boldsymbol{F} + \boldsymbol{M}\ddot{\boldsymbol{\theta}}_{\mathrm{r}} \tag{10}$$

where $\boldsymbol{F}$ is the generalized force vector acting on the torsional vibration system, $\tilde{\theta}$ is the elastic angular acceleration vector

of the torsional vibration system, $\ddot{\theta}_{\mathrm{r}}$ is the rigid body angular acceleration vector of the torsional vibration system, and

$$\ddot{\tilde{\boldsymbol{\theta}}} = \begin{Bmatrix} \ddot{\tilde{\theta}}_1 \\ \ddot{\tilde{\theta}}_2 \\ \ddot{\tilde{\theta}}_3 \end{Bmatrix}, \ddot{\boldsymbol{\theta}}_{\mathrm{r}} = \begin{Bmatrix} \ddot{\theta}_{\mathrm{r}1} \\ \ddot{\theta}_{\mathrm{r}2} \\ \ddot{\theta}_{\mathrm{r}3} \end{Bmatrix}$$

Obviously, the $\boldsymbol{M}\ddot{\theta}_{\mathrm{r}}$ in (10) is the inertial force vector of the torsional vibration system, which can be represented as

$$\boldsymbol{F}_I = \boldsymbol{M}\ddot{\theta}_{\mathrm{r}} \tag{11}$$

In the specific applications, $\boldsymbol{M}$, $\boldsymbol{K}$ and $\boldsymbol{C}$ can usually be obtained by experiments and computations.

### B. CALCULATION OF INERTIAL FORCE

When the end-effector of the manipulator reaches inside the cassette and remains static, the braking acceleration of the manipulator can be approximated as [27]:

$$\ddot{\theta}_{\mathrm{r}i} = \frac{\Delta\dot{\theta}_{\mathrm{r}i}}{T_{\mathrm{s}i}}(1+\tau_{\mathrm{s}i})\left(1-\cos\frac{2\pi}{T_{\mathrm{s}i}}t\right)(i=1,\ 2,\ 3) \tag{12}$$

where, $\Delta\dot{\theta}_{\mathrm{r}i}$ is the changing value of $\dot{\theta}_{\mathrm{r}i}$ during the braking process, and if the braking process is from steady state to rest, so $-\Delta\dot{\theta}_{\mathrm{r}i} = \dot{\theta}_{\mathrm{r}i}0 = \dot{\theta}_{\mathrm{r}i}$, that is to say, the magnitude of $\Delta\dot{\theta}_{\mathrm{r}i}$ is equal to the velocity under the steady state. $T_{\mathrm{s}i}$ is the time during the braking process; $\tau_{\mathrm{s}i}$ is the recovery coefficient of the braking shock, and $0 < \tau_{\mathrm{s}i} < 1$; t is the time spent during the braking process, and $0 \le t \le T_{\mathrm{s}i}$.

Substitute (12) into (11), the inertial force vector of the torsional vibration system can be obtained.

### C. VIBRATION ATTENUATION CHARACTERISTICS

According to the vibration differential (10), the frequency equation of the torsional vibration system can be expressed as

$$\left|\boldsymbol{K} - \omega^2\boldsymbol{M}\right| = \boldsymbol{0} \tag{13}$$

where $\omega$ is the natural frequency of the torsional vibration system of manipulator.

According to (13), the natural frequency of the $i$-order mode of the torsional vibration system, that is $\omega_i$ ($i = 1, 2, 3$), can be calculated. The modal transfer matrix $\boldsymbol{\Phi}$ of the torsional vibration system and the $i$-th order modal coordinate vector corresponding to $\boldsymbol{\Phi}$, that is $\boldsymbol{A}^{(i)}$ ($i = 1, 2, 3$), can be determined by using (13).

According to equation (10), the dynamic response of the torsional vibration system can be obtained by the modal superposition method, which can be expressed as

$$\tilde{\boldsymbol{\theta}} = \sum_{i=1}^{3}\eta_i(t)\boldsymbol{A}^{(i)} \tag{14}$$

where $\eta_i(t)$ is the response of the system under the $i$-th canonical coordinate, which can be obtained by (10) according to the modal analysis method.

Thus, the vibration angular displacement $\tilde{\theta}_{10}$, $\tilde{\theta}_{20}$, $\tilde{\theta}_{30}$ at the end moment of braking process of the torsional vibration system can be calculated by (14). Obviously, the greater the acceleration of the braking process of the torsional vibration system, the greater the inertial force $\boldsymbol{F}_{\mathrm{I}}$ of the system, which leads to the greater the vibration angular displacements $\tilde{\theta}_{10}$, $\tilde{\theta}_{20}$, $\tilde{\theta}_{30}$ of the torsional vibration system of manipulator.

Once the braking process of the torsional vibration system is completed, the external excitations acting on the system no longer exist, and the system can be regarded as a damped multi-degree-of-freedom free vibration system. Under the influence of the damping factors, the vibration of the system will attenuate continuously until the vibration disappears. This vibration phenomenon is the attenuated vibration of the damped multi-degree-of-freedom free vibration system. According to Duhamel's integral method, the formula for calculating the attenuated vibration of the torsional vibration system of the manipulator can be expressed as

$$\begin{aligned}\tilde{\boldsymbol{\theta}}_{\mathrm{m}}(t) = \sum_{i=1}^{3} A^{(i)}e^{-\xi_i\omega_i t}\{(A^{(i)})^{\mathrm{T}}M\tilde{\boldsymbol{\theta}}_0 \times \sin\omega_{di}t \\ + \frac{1}{\omega_{di}}[(A^{(i)})^{\mathrm{T}}M\dot{\tilde{\boldsymbol{\theta}}}_0 + \xi_i\omega_i(A^{(i)})^{\mathrm{T}}M\tilde{\boldsymbol{\theta}}_0]\cos\omega_{di}t\}\end{aligned} \tag{15}$$

where $\tilde{\theta}_{\mathrm{m}}$ is the attenuated vibration angular displacement vector of the system at t-moment; $\omega_{di}$ is the $i$-th order natural frequency with damp; $\xi_i$ is the $i$-th order relative damping coefficient; $\tilde{\theta}_0$ and $\dot{\tilde{\theta}}_0$ are respectively the vibration angular displacement vector and vibration angular velocity vector when the braking process of the torsional vibration system is over, and

$$\begin{aligned}\tilde{\boldsymbol{\theta}}_0 &= \{\tilde{\theta}_{10},\ \tilde{\theta}_{20},\ \tilde{\theta}_{30}\}^{\mathrm{T}} \\ \dot{\tilde{\boldsymbol{\theta}}}_0 &= \{\dot{\tilde{\theta}}_{10},\ \dot{\tilde{\theta}}_{20},\ \dot{\tilde{\theta}}_{30}\}^{\mathrm{T}} \\ \tilde{\boldsymbol{\theta}}_{\mathrm{m}} &= \{\tilde{\theta}_{1\mathrm{m}},\ \tilde{\theta}_{2\mathrm{m}},\ \tilde{\theta}_{3\mathrm{m}}\}^{\mathrm{T}}\end{aligned}$$

where $\tilde{\theta}_{1\mathrm{m}}$, $\tilde{\theta}_{2\mathrm{m}}$ and $\tilde{\theta}_{3\mathrm{m}}$ are respectively the attenuated vibration angular displacements of the big arm, small arm and end arm of the manipulator.

It can be seen from (15) that the larger the attenuation time, the larger the amplitude of the vibration attenuation of the system, and $\tilde{\theta}_{1\mathrm{m}}$, $\tilde{\theta}_{2\mathrm{m}}$, $\tilde{\theta}_{3\mathrm{m}}$ are smaller. When the values of $\tilde{\theta}_{1\mathrm{m}}$, $\tilde{\theta}_{2\mathrm{m}}$, $\tilde{\theta}_{3\mathrm{m}}$ are determined, the attenuation time $t$ can be calculated according to the values required for $\tilde{\theta}_{1\mathrm{m}}$, $\tilde{\theta}_{2\mathrm{m}}$, $\tilde{\theta}_{3\mathrm{m}}$ by using (15).

### D. DYNAMIC ACCURACY OF ROBOT

According to the structural characteristics and working principle of the wafer transfer robot, the dynamic accuracy of the manipulator can be expressed by the vibration displacements $x_{\mathrm{m}}$, $y_{\mathrm{m}}$ at its end. The vibration displacements $x_{\mathrm{m}}$, $y_{\mathrm{m}}$ are in turn related to $\tilde{\theta}_{1\mathrm{m}}$, $\tilde{\theta}_{2\mathrm{m}}$, $\tilde{\theta}_{3\mathrm{m}}$. According to the geometric relationship of the manipulator, the vibration displacements $x_{\mathrm{m}}$, $y_{\mathrm{m}}$ at the end of manipulator can be

expressed as:

$$x_{\mathrm{m}} = l_1\tilde{\theta}_{1\mathrm{m}}\sin\theta_{\mathrm{r}10} + l_2\tilde{\theta}_{2\mathrm{m}}\sin\theta_{\mathrm{r}20} + l_3\tilde{\theta}_{3\mathrm{m}}\sin\theta_{\mathrm{r}30} \quad (16)$$

$$y_{\mathrm{m}} = l_1\tilde{\theta}_{1\mathrm{m}}\cos\theta_{\mathrm{r}10} + l_2\tilde{\theta}_{2\mathrm{m}}\cos\theta_{\mathrm{r}20} + l_3\tilde{\theta}_{3\mathrm{m}}\cos\theta_{\mathrm{r}30} \quad (17)$$

where $\theta_{\mathrm{r}10}$, $\theta_{\mathrm{r}20}$ and $\theta_{\mathrm{r}30}$ are respectively the angles between rods OA, AB, BC and $X$-axis at the moment when the braking process of the torsional vibration system is over.

When the manipulator of the $R$-$\theta$ wafer transfer robot loads and unloads wafers, to meet the required accuracy requirements for loading and unloading wafers, the manipulator should wait for a certain period after the end-effector of the manipulator reaches inside the CST and remains static so that the vibration displacements $x_{\mathrm{m}}$ and $y_{\mathrm{m}}$ at the end of the manipulator are attenuated continuously until the dynamic accuracy of the system meets the required values. When the dynamic accuracy of the robot meets the required accuracy for loading and unloading wafers, the manipulator of the robot is allowed to load and unload the wafers.

## IV. SCHEDULING ANALYSIS AND OPTIMIZING

### A. PROBLEM DESCRIPTION

The robot goes through the process from the steady operation phase to the braking phase during loading and unloading wafers. The process by which the robot goes from the steady motion phase to the braking phase is the deceleration motion, and during this transition, the manipulator will generate the inertial force. The value of the generated inertial force is related not only to the steady motion speed but also to the transition time from the steady motion phase to the braking phase. The smaller the transition time is, the larger the inertial force. The greater the inertial force is, the greater the vibration of the robot under the action of the inertial force, and the lower the dynamic accuracy of the robot. The dynamic accuracy of the manipulator of the robot will directly affect the quality of wafer transfer. Obviously, to ensure the transferring and processing qualities of the wafers, the vibration of the manipulator of the robot during loading and unloading wafers has to be kept within certain limits. According to the working principle of the manipulator of the robot and mechanical vibration theory, once the braking process of the manipulator of the robot is completed, the external excitations acting on the manipulator no longer exist. At this moment, the manipulator can be regarded as a damped multi-degree-of-freedom free vibration system. Under the influence of damping factors, the vibration of the system continues to attenuate with the passage of time. When the vibration amplitudes are within the permitted range after a certain period, the manipulator of the robot is allowed to load and unload the wafers. In summary, when the end-effector of the manipulator enters the processing module $\mathrm{PM}_i$ or load lock for loading and unloading wafers, the manipulator needs to wait for a certain amount of time so that the vibration amplitudes of the system are within the permitted range. Thus, it is necessary to consider the dynamic accuracy constraints of the manipulator of the robot when the single-arm cluster tools are scheduled and controlled to satisfy the transferring and processing qualities of the wafers. Meanwhile, for some wafer fabrication processes, such as low pressure chemical-vapor deposition (LPCVD), there are strict wafer residence time constraints, which require wafers to be removed within a limited time after they are processed in one of the processing modules in the cluster tools. Otherwise the chemical gases and high temperatures in the processing module can damage the wafers. Therefore, the effect of the wafer residency constraints needs to be considered when single-arm cluster tools are scheduled and controlled in this case.

However, for single-arm cluster tools, any waiting times of the manipulator of the robot affect the workload of the process steps. Thus, for single-arm cluster tools with dynamic accuracy constraints and wafer residency time constraints, it is necessary to regulate the waiting times of the manipulator of the robot and offset the wafer residency time delay as much as possible to optimize the scheduling of single-arm cluster tools and ensure wafer quality.

In order to solve the problems above, we divide this class of problems into two stages:

(1) The first stage determines the minimum waiting times for the manipulator of robot to wait for loading and unloading wafers in each processing module and load lock under steady state when the dynamic accuracy constraints is considered.

(2) The second stage achieves the scheduling optimization and control of single-arm cluster tools with dynamic accuracy constraints and wafer residency time constraints.

### B. LIST OF SYMBOLS AND VARIABLES

The list of symbols and variables are used in the article are shown in the Nomenclature section.

### C. CONDITIONS FOR DYNAMIC ACCURACY CONSTRAINTS ON MANIPULATOR

In the process of loading and unloading wafers, the manipulator of the robot is affected by the self-excitation inertial force since the manipulator runs from the steady state to the braking state. Under the action of inertial force, forced vibration will be produced in the manipulator and affect the dynamic accuracy of the manipulator during loading and unloading wafers, which in turn affects the transferring and processing qualities of the wafers. Therefore, to ensure the transferring and processing qualities of wafers, the vibration amplitude of the manipulator should be controlled within the permitted range to meet the requirements of dynamic accuracy when the wafers are loaded and unloaded.

In this paper, we determine the minimum waiting time for the manipulator for loading and unloading wafers in each processing module and the load lock under dynamic accuracy constraints. That is, according to the quality requirements of the wafers, we apply the above method to determine the minimum waiting times for the manipulator for loading and

unloading wafers at the $i$-th processing module $PM_i$ or load lock under a steady schedule. In the subsequent scheduling optimization and control of the single-arm cluster tools, the manipulator should be scheduled strictly in accordance with the preset minimum waiting times $T_{Wi1min}$ and $T_{Wi2min}$.

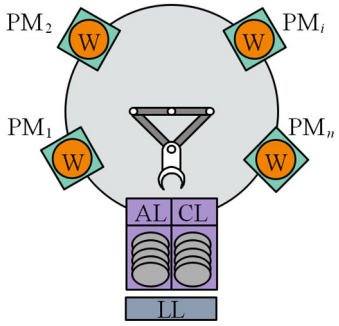


**FIGURE 3.** Single-arm cluster tools.

### D. SCHEDULING ANALYSIS

The single-arm cluster tools for wafer fabrication generally consist of several processing modules (PMs), tow load locks (LLs), an aligner module (AL), a cooler module (CL), and a single-arm robot, as shown in Figure 3 [28]. The modules are distributed in a radial direction and are controlled by a computer. The raw wafers to be processed are unloaded from the load lock, visit the PMs in sequence according to the process recipe, enter the CL to be cooled, and return to the load lock after completing the process. The single-arm cluster tools wafer fabrication system is a typical discrete-event dynamic system. Since Petri net can provide a good description of concurrent events, the asynchronous concurrent events and the logical relationships of each process in the wafer processing of single-arm cluster tools, it is used here, as shown in Figure 4. Without loss of generality, let the initial state of the system $M_0(p_i) = m_i$ $(i \in \mathbf{N}_n)$, $M_0(r) = 1$, and let $M_0(p_0) = \infty$ to ensure that there are always wafers to be processed in each PM of the system.

The single-arm cluster tools process wafers in three states: initial transient state, steady state and termination state. The initial state of the system is idle, and the initial transient state starts when the manipulator of the robot unloads the first unprocessed wafer from the load lock. The system enters the steady state when all PMs of the system have wafers processed at the same time. The system operates periodically in a steady state. If the parallel modules of the system are not considered, the steady operation of the manipulator of the single-arm robot requires the execution of the following sequences, where the brackets represent the time spent for each action by the manipulator of the single-arm cluster tools: Move from $PM_1$ to $PM_n$ and wait $(T_{M1n} + T_{Wn2}) \rightarrow$ Unload wafer from $PM_n$ $(T_{Sn2}) \rightarrow$ Move to LL and wait $(T_{Mn0} + T_{W01}) \rightarrow$ Load wafer into LL $(T_{S01}) \rightarrow$ Move to $PM_{n-1}$ and wait $(T_{M0(n-1)} + T_{W(n-1)2}) \rightarrow$ Unload wafer from $PM_{n-1}$ $(T_{S(n-1)2}) \rightarrow$ Move to $PM_n$ and wait $(T_{M(n-1)n} + T_{Wn1}) \rightarrow$ Load wafer into $PM_n$ $(T_{Sn1}) \rightarrow$ Move to $PM_{n-2}$ and wait $(T_{Mn(n-2)} + T_{W(n-2)1}) \rightarrow \ldots \rightarrow$ Move from $PM_{i+2}$ to $PM_i$ and wait $(T_{M(i+2)i} + T_{Wi2}) \rightarrow$ Unload wafer from $PM_i$ $(T_{Si2}) \rightarrow$ Move to $PM_{i+1}$ and wait $(T_{Mi(i+1)} + T_{W(i+1)1}) \rightarrow$ Load wafer into $PM_{i+1}$ $(T_{S(i+1)1}) \rightarrow$ Move to $PM_{i-1}$ and wait $(T_{M(i+1)(i-1)} + T_{W(i-1)2}) \rightarrow \ldots \rightarrow$ Unload wafer from the LL$(T_{S02}) \rightarrow$ Move to $PM_1$ and wait $(T_{M01} + T_{W11}) \rightarrow$ Load wafer into $PM_1$ $(T_{S11})$.

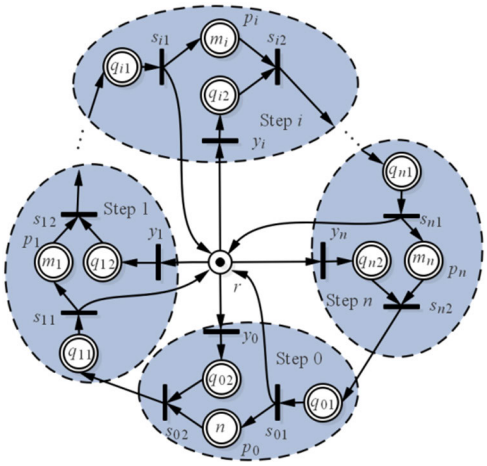


**FIGURE 4.** The resource-oriented Petri net model for single-arm tools.

According to the steady operation sequences of the manipulator of the robot described above, when the system is running steadily, the time $T_Z$ that the manipulator requires to run a cycle can be expressed as

$$T_Z = T_{Z1} + T_{Z2} \tag{18}$$

where $T_{Z1}$ is the total action time that the manipulator requires during a steady operation cycle, $T_{Z2}$ is the total waiting time that the manipulator requires during a steady operation cycle, and

$$T_{Z1} = T_{M1n} + T_{Mn0} + T_{M0(n-1)} + \sum_{i=0}^{n-2} T_{M(i+2)i} + \sum_{i=0}^{n-1} T_{Mi(i+1)} + \sum_{i=0}^{n} T_{Si1} + \sum_{i=0}^{n} T_{Si2} \tag{19}$$

$$T_{Z2} = \sum_{i=0}^{n} T_{Wi1} + \sum_{i=0}^{n} T_{Wi2} \tag{20}$$

The total action time $T_{Z1}$ of the manipulator is determined by the processing technology of wafers and $T_{Z1}$ is a constant value. So the total waiting time $T_{Z2}$ of the manipulator will varies with the time $T_Z$. Once $T_Z$ is determined, the total waiting time $T_{Z2}$ can be calculated by (18).

According to the Petri net model shown in Figure 4, the following sequence of operations is required for the wafer to complete the first process, with the time spent on the action in parentheses: Unload wafer from $PM_1$ and move it to $PM_2$ $(T_{S12} + T_{M12}) \rightarrow$ Wait to load wafer into $PM_2$

($T_{W21}$) → Load wafer into $PM_2$ ($T_{S21}$) → Move from $PM_2$ to LL with no load($T_{M20}$) → Wait to unload wafer from LL ($T_{W02}$) → Move to $PM_1$ after unloading wafer alignment from LL ($T_{C0} + T_{M01}$) → Wait to load wafer into $PM_1$ ($T_{W11}$) → Load wafer into $PM_1$ ($T_{S11}$) → Process wafer in $PM_1$ ($T_{P1}$).

So the equation for calculating the production cycle for the completion of the first process by the single-arm cluster tools can be expressed as

$$T_{L1} = \frac{1}{m_1}[T_{P1} + T_{C0} + T_{S11} + T_{S12} + T_{S21} + T_{M01} + T_{M12} + T_{M20} + T_{W02} + T_{W11} + T_{W21}] \quad (21)$$

According to the Petri net model shown in Figure 4, the following sequence of operations is required for the wafer to complete the $i$-th process, with the time spent on the action in parentheses: Unload wafer from $PM_i$ and move it to $PM_{i+1}$ ($T_{Si2} + T_{Mi(i+1)}$) → Wait to load wafer in $PM_{i+1}$ ($T_{W(i+1)1}$) → Load wafer into $PM_{i+1}$ ($T_{S(i+1)1}$) → Move from $PM_{i+1}$ to $PM_{i-1}$ with no load ($T_{M(i+1)(i-1)}$) → Wait to unload wafer from $PM_{i-1}$ ($T_{W(i-1)2}$) → Unload wafer from $PM_{i-1}$ and move it to $PM_i$ ($T_{S(i-1)2} + T_{M(i-1)i}$) → Wait to load wafer into $PM_i$ ($T_{Wi1}$) → Load wafer into $PM_i$ ($T_{Si1}$) → Process wafer in $PM_i$ ($T_{Pi}$).

So the lower bound of the production cycle for the completion of the $i$-th process by the single-arm cluster tools can be written as

$$T_{Li} = \frac{1}{m_i}[T_{Pi} + T_{S(i-1)2} + T_{Si1} + T_{Si2} + T_{S(i+1)1} + T_{M(i-1)i} + T_{Mi(i+1)} + T_{M(i+1)(i-1)} + T_{W(i-1)2} + T_{Wi1} + T_{W(i+1)1}] \quad (22)$$

According to the Petri net model shown in Figure 4, the following sequence of operations is required for the wafer to complete the $n$-th process, with the time spent on the action in parentheses: Unload wafer from $PM_n$ and move it to LL ($T_{Sn2} + T_{Mn0}$) → Wait to load wafer into LL ($T_{W01}$) → Load wafer into the LL ($T_{S01}$) → Move from LL to $PM_{n-1}$ with no load ($T_{M0(n-1)}$) → Wait to unload wafer from $PM_{n-1}$ ($T_{W(n-1)2}$) → Unload wafer from $PM_{n-1}$ and move it to $PM_n$ ($T_{S(n-1)2} + T_{M(n-1)n}$) → Wait to load wafer into $PM_n$ ($T_{Wn1}$) → Load wafer into $PM_n$ ($T_{Sn1}$) → Process wafer in $PM_n$ ($T_{Pn}$).

So the lower bound of the production cycle for the completion of the $n$-th process by the single-arm cluster tools can be obtained as

$$T_{Ln} = \frac{1}{m_n}[T_{Pn} + T_{S(n-1)2} + T_{Sn1} + T_{Sn2} + T_{S01} + T_{M(n-1)n} + T_{Mn0} + T_{M0(n-1)} + T_{W(n-1)2} + T_{Wn1} + T_{W01}] \quad (23)$$

In the normal case, when a single-arm cluster tools in steady operation is scheduled using the backward strategy, the time required to run a cycle of the manipulator and the production cycles of all processes are equal to the system cycle $T_P$ under the steady schedule of single-arm cluster tools [29], namely

$$T_{L1} = \cdots = T_{Li} = \cdots = T_{Ln} = T_Z = T_P \quad (24)$$

After the system cycle time is determined, the production cycle time of each process can meet the requirement of (24) by reasonably adjusting the waiting time of each process when the maximum value of the sum of waiting time for each process can be expressed as [29]

$$T_{W1max} = m_1 T_P - (T_{C0} + T_{S11} + T_{S12} + T_{S21} + T_{M01} + T_{M12} + T_{M20}) \quad (25)$$

$$T_{Wimax} = m_i T_P - [T_{S(i-1)2} + T_{Si1} + T_{Si2} + T_{S(i+1)1} + T_{M(i-1)i} + T_{Mi(i+1)} + T_{M(i+1)(i-1)}] \quad (26)$$

$$T_{Wnmax} = m_n T_P - [T_{S(n-1)2} + T_{Sn1} + T_{Sn2} + T_{S01} + T_{M(n-1)n} + T_{Mn0} + T_{M0(n-1)}] \quad (27)$$

Similarly, when the system cycle time is determined and the production cycle time of each process satisfies the requirements of (24), the actual residence time of the wafer during processing in each process can be obtained from (25), (18), (21), (22) and (23), namely

$$T_{P1} = m_1[T_{M1n} + T_{Mn0} + T_{M0(n-1)} + \sum_{i=0}^{n-2} T_{M(i+2)i} + \sum_{i=0}^{n-1} T_{Mi(i+1)} + \sum_{i=0}^{n} T_{Si1} + \sum_{i=0}^{n} T_{Si2} + \sum_{i=0}^{n} T_{Wi1} + \sum_{i=0}^{n} T_{Wi2}] - (T_{C0} + T_{S11} + T_{S12} + T_{S21} + T_{M01} + T_{M12} + T_{M20} + T_{W02} + T_{W11} + T_{W21}) \quad (28)$$

$$T_{Pi} = m_i[T_{M1n} + T_{Mn0} + T_{M0(n-1)} + \sum_{i=0}^{n-2} T_{M(i+2)i} + \sum_{i=0}^{n-1} T_{Mi(i+1)} + \sum_{i=0}^{n} T_{Si1} + \sum_{i=0}^{n} T_{Si2} + \sum_{i=0}^{n} T_{Wi1} + \sum_{i=0}^{n} T_{Wi2}] - (T_{S(i-1)2} + T_{Si1} + T_{Si2} + T_{S(i+1)1} + T_{M(i-1)i} + T_{Mi(i+1)} + T_{M(i+1)(i-1)} + T_{W(i-1)2} + T_{Wi1} + T_{W(i+1)1}) \quad (29)$$

$$T_{Pn} = m_n[T_{M1n} + T_{Mn0} + T_{M0(n-1)} + \sum_{i=0}^{n-2} T_{M(i+2)i} + \sum_{i=0}^{n-1} T_{Mi(i+1)} + \sum_{i=0}^{n} T_{Si1} + \sum_{i=0}^{n} T_{Si2} + \sum_{i=0}^{n} T_{Wi1} + \sum_{i=0}^{n} T_{Wi2}] - (T_{S(n-1)2} + T_{Sn1} + T_{Sn2} + T_{S01} + T_{M(n-1)n} + T_{Mn0} + T_{M0(n-1)} + T_{W(n-1)2} + T_{Wn1} + T_{W01}) \quad (30)$$

### E. MATHEMATICAL PROGRAMMING MODEL

#### 1) DECISION VARIABLES

In (18), the time $T_Z$ that the manipulator requires to run a cycle is composed of the total action time $T_{Z1}$ and the total waiting time $T_{Z2}$ in a steady operation cycle. From (19), it can be seen that the total action time $T_{Z1}$ is determined by the system and the processing technology of wafers, and the value of $T_{Z1}$ is generally constant. The total waiting time $T_{Z2}$ of the manipulator in a steady operation cycle is an unknown quantity that needs to be determined, so the waiting times $T_{Wi1}$ for the manipulator to load wafers into $PM_i$ or the load lock and $T_{Wi2}$ for the manipulator to unload wafers from $PM_i$ or the load lock are taken as the decision variables, where $\{i \in 0, 1, 2, \cdots, n\}$.

#### 2) OBJECTIVES

To make the system cycle time under the steady schedule of the single-arm cluster tools meet the preset requirements and offset the wafer residency time delay as much as possible to ensure the balance of the system residency time delay, an objective function is determined here. The objective function is used to minimize the sum of the wafer residency time delay in each process.

#### 3) CONSTRAINTS

To ensure the quality of wafers, the dynamic accuracy of the manipulator of the robot during loading and unloading wafers has to meet certain requirements. To meet the requirements for transferring and processing quality of wafers, the dynamic accuracy of the manipulator during loading and unloading wafers can be ensured by limiting the waiting times of the manipulator according to the intrinsic relationship between the waiting times of the manipulator during loading and unloading wafers and the dynamic accuracy. In the meantime, for some wafer fabrication processes, such as low pressure chemical-vapor deposition (LPCVD), there are strict wafer residency time constraints. When a wafer is processed in one of the processing modules in the cluster tools, it must be removed within the limited time. Otherwise, the chemical gases and high temperature in the processing module will damage the wafer.

Thus, the scheduling question for the single-arm cluster tools is a single objective scheduling question with dynamic accuracy constraints and wafer residency time constraints. Then, a linear programming model is established for the addressed scheduling problem as follows.

$$\text{Min} \sum_{i=1}^{n} \Delta T_i \tag{31}$$

$$\Delta T_i = T_{Pi} - T_{Pi\min} \tag{32}$$

$$T_{Pi\min} \le T_{Pi} \le T_{Pi\max}, i \in \{1, \ 2, \ \cdots, \ n\} \tag{33}$$

$$T_{Wi1} \ge T_{Wi1\min}, i \in \{0, \ 1, \ 2, \ \cdots, \ n\} \tag{34}$$

$$T_{Wi2} \ge T_{Wi2\min}, i \in \{0, \ 1, \ 2, \ \cdots, \ n\} \tag{35}$$

$$T_{W02} + T_{W11} + T_{W21} \le T_{W1\max} \tag{36}$$

$$T_{W(i-1)2} + T_{Wi1} + T_{W(i+1)1} \le T_{Wi\max}, i \in \{2, \ \cdots, \ (n-1)\} \tag{37}$$

$$T_{W(n-1)2} + T_{Wn1} + T_{W01} \le T_{Wn\max} \tag{38}$$

$$\sum_{i=0}^{n} T_{Wi1} + \sum_{i=0}^{n} T_{Wi2} = T_P - T_{Z1} \tag{39}$$

Objective (31) indicates that the sum of the wafer residency time delays in each process is minimized to ensure that the total waiting time of the manipulator of robot in a steady operation cycle can be used to offset the wafer residency time delay.

Constraint (32) calculates the value of wafer residency time delay for the $i$-th process of the single-arm cluster tools; Constraint (33) indicates the constraint condition on the actual residency time of the wafer which is being processed in $PM_i$; Constraint (34) denotes the minimum waiting time constraint for the manipulator to wait for loading wafers into $PM_i$ or load lock; Constraint (35) denotes the minimum waiting time constraint for the manipulator to wait for unloading wafers from $PM_i$ or load lock; Constraint (36) denotes the total wait time constraint for the manipulator in the first process. Constraint (37) denotes the total waiting time constraint for the manipulator in the $i$-th process; Constraint (38) denotes the total waiting time constraint for the manipulator in the $n$-th process; Constraint (39) denotes the total waiting time constraint for the manipulator in a steady operation cycle. Obviously, (34)- (39) denote the constraints that should be satisfied by the waiting time allocation of the manipulator, respectively.

## V. EXPERIMENT

In this section we verify the correctness of the developed model by using cluster tools as an example. In this study, the linear programming model established above is solved by using Python as the programming language and CPLEX as the solver.

CPLEX has been widely recognized by the academic community as a type of commercial optimization software with excellent performance in solving. It is broadly known by the academic community. Therefore, we use IBM ILOG CPLEX (version 22.1.0) as the LP solver in our experiments. Experiments were performed on a laptop with Windows 10 as operating system, processor eight Intel (R) Core (TM) i7-10510U CPU @ 1.80 GHz and 64 Go of RAM. ''Float over text'' should not be selected.

### A. EXAMPLE 1

#### 1) SCHEDULING EXPERIMENTS CONSIDERING DYNAMIC ACCURACY CONSTRAINTS

There are four processing modules in this cluster tools. The wafer fabrication flow pattern is (1, 1, 1, 1), and the wafer processing sequence in cluster tools is PM1→PM2→PM3 →PM4. The processing parameters required in Example 1 are shown in Table 1.

**TABLE 1.** Processing parameters required in example 1.

| Parameter | Numericl value | Unit |
|---|---|---|
| $T_{\mathrm{P}}$ | 110 | s |
| $T_{\mathrm{Z1}}$ | 90 | s |
| $T_{\mathrm{C0}}$ | 10 | s |
| $T_{\mathrm{S}i1}$ | {3, 3, 3, 3, 3} | s |
| $T_{\mathrm{S}i2}$ | {3, 3, 3, 3, 3} | s |
| $T_{\mathrm{P}i\mathrm{min}}$ | {90, 80, 95, 90} | s |
| $T_{\mathrm{W}i1\mathrm{min}}$ | {1, 1.5, 1, 2, 1.7} | s |
| $T_{\mathrm{W}i2\mathrm{min}}$ | {1, 1.5, 1, 2, 1.7} | s |

The time for the manipulator of the $R$-$\theta$ wafer transfer robot to move from $\mathrm{PM}_i$ to $\mathrm{PM}_j$ can be written as

$$T_{\mathrm{M}ij} = \begin{pmatrix} 0 & 0.7 & 1.2 & 1.2 & 0.7 \\ 0.7 & 0 & 0.5 & 1 & 1.5 \\ 1.2 & 0.5 & 0 & 0.5 & 1 \\ 1.2 & 1 & 0.5 & 0 & 0.5 \\ 0.7 & 1.5 & 1 & 0.5 & 0 \end{pmatrix}$$

where the rows denote $\mathrm{PM}_i$ and the columns denote $\mathrm{PM}_j$.

The CPLEX solver obtained the experimental results in 0.91 s. The results show that the manipulator waiting time allocation scheme is $T_{\mathrm{W}i1} = \{1, 1.5, 1, 18.4, 1.7\}$ and $T_{\mathrm{W}i2} = \{1, 1.5, 1, 7.8, 41.2\}$. When the allocation scheme is adopted, the sum of the wafer residency time delay values in each process is minimized and the minimum value is 71.1 s.

#### 2) SCHEDULING EXPERIMENTS WITHOUT CONSIDERING DYNAMIC ACCURACY CONSTRAINTS

If we do not consider the effect of dynamic accuracy constraints in our scheduling experiments, the minimum waiting time $T_{\mathrm{W}i1\mathrm{min}}$ for the manipulator to wait to load a wafer into $\mathrm{PM}_i$ or the load lock and the minimum waiting time $T_{\mathrm{W}i2\mathrm{min}}$ for the manipulator to wait to unload a wafer from $\mathrm{PM}_i$ or the load lock are all zero. The rest of the parameter settings are the same as when dynamic accuracy constraints are considered.

The CPLEX solver obtained the experimental results in 0.79 s. The results show that the manipulator waiting time allocation scheme is $T_{\mathrm{W}i1} = \{0, 0, 0, 17.4, 0\}$ and $T_{\mathrm{W}i2} = \{0, 0, 0, 7, 48.2\}$. When the allocation scheme is adopted, the sum of the wafer residency time delay values in each process is minimized and the minimum value is 67.6 s.

### B. EXAMPLE 2

#### 1) SCHEDULING EXPERIMENTS CONSIDERING DYNAMIC ACCURACY CONSTRAINTS

There are four processing modules in the cluster tools, but there are only three processes in total, with $\mathrm{PM}_2$ and $\mathrm{PM}_3$ being the parallel modules for the second process. The wafer fabrication flow pattern is (1, 2, 1) and the wafer processing sequence in cluster tools is $\mathrm{PM}_1 \rightarrow \mathrm{PM}_2$ (or $\mathrm{PM}_3$) $\rightarrow \mathrm{PM}_4$. The processing parameters required in Example 2 are shown in Table 2.

**TABLE 2.** Processing parameters required in example 2.

| Parameter | Numericl value | Unit |
|---|---|---|
| $T_{\mathrm{P}}$ | 91 | s |
| $T_{\mathrm{Z1}}$ | 78 | s |
| $T_{\mathrm{C0}}$ | 15 | s |
| $T_{\mathrm{S}i1}$ | {4, 4, 4, 4} | s |
| $T_{\mathrm{S}i2}$ | {4, 4, 4, 4} | s |
| $T_{\mathrm{P}i\mathrm{min}}$ | {85, 120, 100} | s |
| $T_{\mathrm{W}i1\mathrm{min}}$ | {1, 1.2, 2.3, 1.6} | s |
| $T_{\mathrm{W}i2\mathrm{min}}$ | {1, 1.2, 1.9, 1.3} | s |

The time for the manipulator of the $R$-$\theta$ wafer transfer robot to move from $\mathrm{PM}_i$ to $\mathrm{PM}_j$ can be written as

$$T_{\mathrm{M}ij} = \begin{pmatrix} 0 & 0.4 & 0.8 & 0.8 & 0.4 \\ 0.4 & 0 & 0.3 & 0.6 & 0.9 \\ 0.8 & 0.3 & 0 & 0.3 & 0.6 \\ 0.8 & 0.6 & 0.3 & 0 & 0.3 \\ 0.4 & 0.9 & 0.6 & 0.3 & 0 \end{pmatrix}$$

where the rows denote $\mathrm{PM}_i$ and the columns denote $\mathrm{PM}_j$.

The CPLEX solver obtained the experimental results in 0.76 s. The results show that the manipulator waiting time allocation scheme is $T_{\mathrm{W}i1} = \{1, 1.2, 11.7, 1.6\}$ and $T_{\mathrm{W}i2} = \{1, 1.2, 1.9, 66.2\}$. When the allocation scheme is adopted, the sum of the wafer residency time delay values in each process is minimized and the minimum value is 43.8 s.

#### 2) SCHEDULING EXPERIMENTS WITHOUT CONSIDERING DYNAMIC ACCURACY CONSTRAINTS

If we do not consider the effect of dynamic accuracy constraints in our scheduling experiments, the minimum waiting time $T_{\mathrm{W}i1\mathrm{min}}$ for the manipulator to wait to load a wafer into $\mathrm{PM}_i$ or the load lock and the minimum waiting time $T_{\mathrm{W}i2\mathrm{min}}$ for the manipulator to wait to unload a wafer from $\mathrm{PM}_i$ or the load lock are all zero. The rest of the parameter settings are the same as when dynamic accuracy constraints are considered.

The CPLEX solver obtained the experimental results in 0.46 s. The results show that the manipulator waiting time allocation scheme is $T_{\mathrm{W}i1} = \{0, 9.4, 0, 0\}$ and $T_{\mathrm{W}i2} = \{0, 0, 71.9, 0\}$. When the allocation scheme is adopted, the sum of the wafer residency time delay values in each process is minimized and the minimum value is 39.3 s.

### C. EXAMPLE 3

#### 1) SCHEDULING EXPERIMENTS CONSIDERING DYNAMIC ACCURACY CONSTRAINTS

There are four processing modules in this cluster tools. The wafer fabrication flow pattern is (1, 1, 1, 1), and the wafer processing sequence in cluster tools is PM1→PM2→PM3 →PM4. The processing parameters required in Example 3 are shown in Table 3.

**TABLE 3. Processing parameters required in example 3.**

| Parameter | Numericl value | Unit |
|---|---|---|
| $T_{\mathrm{P}}$ | 95 | s |
| $T_{\mathrm{Z1}}$ | 80 | s |
| $T_{\mathrm{C0}}$ | 15 | s |
| $T_{\mathrm{S}i1}$ | {3, 3, 3, 3, 3} | s |
| $T_{\mathrm{S}i2}$ | {3, 3, 3, 3, 3} | s |
| $T_{\mathrm{P}i\min}$ | {90, 80, 95, 90} | s |
| $T_{\mathrm{W}i1\min}$ | {1, 1.2, 2.3, 1.6, 1.5} | s |
| $T_{\mathrm{W}i2\min}$ | {1, 1.2, 1.9, 1.3, 1.5} | s |

The time for the manipulator of the $R$-$\theta$ wafer transfer robot to move from $\mathrm{PM}_i$ to $\mathrm{PM}_j$ can be written as

$$T_{\mathrm{M}ij} = \begin{pmatrix} 0 & 0.4 & 0.8 & 0.8 & 0.4 \\ 0.4 & 0 & 0.3 & 0.6 & 0.9 \\ 0.8 & 0.3 & 0 & 0.3 & 0.6 \\ 0.8 & 0.6 & 0.3 & 0 & 0.3 \\ 0.4 & 0.9 & 0.6 & 0.3 & 0 \end{pmatrix}$$

where the rows denote $\mathrm{PM}_i$ and the columns denote $\mathrm{PM}_j$.

According to the experimental results, there is no feasible scheduling solution in this case.

### 2) SCHEDULING EXPERIMENTS WITHOUT CONSIDERING DYNAMIC ACCURACY CONSTRAINTS

If we do not consider the effect of dynamic accuracy constraints in our scheduling experiments, the minimum waiting time $T_{\mathrm{W}i1\min}$ for the manipulator to wait to load a wafer into $\mathrm{PM}_i$ or the load lock and the minimum waiting time $T_{\mathrm{W}i2\min}$ for the manipulator to wait to unload a wafer from $\mathrm{PM}_i$ or the load lock are all zero. The rest of the parameter settings are the same as when dynamic accuracy constraints are considered.

The CPLEX solver obtained the experimental results in 0.62 s. The results show that the manipulator waiting time allocation scheme is $T_{\mathrm{W}i1} = \{0, 0, 7.3, 0\}$, $T_{\mathrm{W}i2} = \{0, 0, 12, 55.8\}$. When the allocation scheme is adopted, the sum of the wafer residency time delay values in each process is minimized and the minimum value is 55.1 s.

Examples 1 and 2 show that the sum of wafer residence time delays in each process without considering the dynamic accuracy constraint is less than that when considering the dynamic accuracy constraint. It can be seen from example 3 that the feasible scheduling solution exists when the dynamic accuracy constraint is not considered while the feasible scheduling solution does not exist when the dynamic accuracy constraint is considered. Obviously, the scheduling scheme without considering the dynamic accuracy constraint is not the same as that when considering the dynamic accuracy constraint. However, the dynamic accuracy constraint of the robot is objective. When the scheduling and control of cluster tools is performed according to the scheduling scheme without considering the dynamic accuracy constraint, the accuracy requirements of wafer processing and the expected scheduling effect may not be met.

Meanwhile, the calculation time of the CPLEX solvers in the above examples is less than 1 s. This means that the mathematical programming model established in this paper can find an optimal solution in reasonable time for real cases.

## VI. CONCLUSION

Cluster tools are high-precision automated and integrated equipment used for processing wafers. Effective scheduling and control of cluster tools is critical to increase the production efficiency and improve the product quality of wafers. As the key part of integrated circuit equipment, the dynamic accuracy of the manipulator of wafer transfer robot is an important constraint that directly affects the transferring and processing quality of wafers. Therefore, it is necessary to consider the influence of dynamic accuracy constraints when cluster tools are scheduled and controlled.

In this paper, the single-arm cluster tools are taken as the research object. The differential equations of torsional vibration of the manipulator of the $R$-$\theta$ robot are constructed by applying Lagrangian equation, and the expression of the inertial forces of the manipulator is derived. Based on the vibration equations, the torsional vibration mechanism of the manipulator is studied and the vibration attenuation characteristics of the manipulator are analyzed. Meanwhile, the intrinsic relationships between the dynamic accuracy of the manipulator during loading and unloading wafers and the waiting times of the manipulator are explored, and the calculation method of the minimum waiting times when meeting the dynamic accuracy requirements of the manipulator is determined. Then the two-stage approach is proposed for the scheduling optimization and control of single-arm cluster tools. The first stage determines the minimum waiting times of the manipulator based on the intrinsic relationships between the dynamic accuracy of manipulator and the waiting times of manipulator. The second stage establishes the mathematical programming model and achieves the scheduling and control of single-arm cluster tools with dynamic accuracy constraints and wafer residency time constraints. Finally, the experimental study shows that the proposed two-stage approach is effective and adaptive. Future work will further study the scheduling and control of cluster tools with complex constraints by improving the kinematics and dynamics of the wafer transfer robot manipulator.

## REFERENCES

[1] S. Oh-Hara, K. Hirata, and Y. Ohta, "A switching gain scheduled approach for wafer transfer robots and its experimental evaluations," in *Proc. Amer. Control Conf.*, Minneapolis, Minnesota, 2006, pp. 3898–3903.

[2] Y. Liu, H. Han, L. Sun, K. Li, and T. Liu, "An integrated system of detecting end-effector motion states and wafer stick-slip on a wafer transfer robot," in *Proc. IEEE Int. Conf. Mechatronics Autom.*, Harbin, China, Aug. 2016, pp. 2570–2575.

[3] X. Yu, Y. Zhao, C. Wang, and M. Tomizuka, "Trajectory planning for robot manipulators considering kinematic constraints using probabilistic roadmap approach," *J. Dyn. Syst., Meas., Control*, vol. 139, no. 2, Feb. 2017, Art. no. 021001.

[4] Y. Liu, Y. Hu, and X. Zheng, "Stable and accurate trajectory control technology for the wafer transfer robot," in *Proc. IEEE Int. Conf. Inf. Autom.*, Harbin, China, Jun. 2010, pp. 1336–1340.
[5] M. D. Duong and K. Terashima, "Development of vibration suppression GUI tool based input preshaping control and its applications to wafer transfer robot and gantry loader systems," in *Proc. Eur. Control Conf. (ECC)*, Budapest, Hungary, Aug. 2009, pp. 5027–5032.
[6] Z. Wang, C. Wang, and M. Tomizuka, "Active wide-band vibration rejection for semiconductor manufacturing robots," in *Proc. ASME Dynamic Syst. Control Conf.*, Columbus, Ohio, 2015, pp. 1–8.
[7] W. Aribowo, T. Yamashita, K. Terashima, Y. Masui, T. Saeki, T. Kamigaki, and H. Kawamura, "Vibration control of semiconductor wafer transfer robot by building an integrated tool of parameter identification and input shaping," in *Proc. 18th World Congr. Int. Fed. Autom. Control*, Milano, Italy, 2011, pp. 14367–14373.
[8] Y. Liu, Y. Cao, L. Sun, and X. Zheng, "Vibration suppression for wafer transfer robot during trajectory tracking," in *Proc. IEEE Int. Conf. Mechatronics Autom.*, Aug. 2010, pp. 741–746.
[9] M. H. Korayem, H. Ghariblu, and A. Basu, "Dynamic load-carrying capacity of mobile-base flexible joint manipulators," *Int. J. Adv. Manuf. Technol.*, vol. 25, nos. 1–2, pp. 62–70, Jan. 2005.
[10] M. H. Korayem and A. Nikoobin, "Maximum payload for flexible joint manipulators in point-to-point task using optimal control approach," *Int. J. Adv. Manuf. Technol.*, vol. 38, nos. 9–10, pp. 1045–1060, Sep. 2008.
[11] M. Korayem, A. Heidari, and A. Nikoobin, "Maximum allowable load of flexible mobile manipulators using finite element approach," *Int. J. Adv. Manuf. Technol.*, vol. 36, nos. 9–10, pp. 1010–1021, 2008.
[12] H. Ma, Q. Zhou, H. Li, and R. Lu, "Adaptive prescribed performance control of a flexible-joint robotic manipulator with dynamic uncertainties," *IEEE Trans. Cybern.*, vol. 52, no. 12, pp. 12905–12915, Dec. 2022.
[13] Y. Lu, Y. Qiao, C. Pan, Y. Chen, N. Wu, Z. Li, and B. Liu, "Modeling and control for deadlock-free operation of single-arm cluster tools with concurrently processing multiple wafer types via Petri net," *IEEE Access*, vol. 9, pp. 70868–70883, 2021.
[14] J. Wang, P. Gao, P. Zheng, J. Zhang, and W. H. Ip, "A fuzzy hierarchical reinforcement learning based scheduling method for semiconductor wafer manufacturing systems," *J. Manuf. Syst.*, vol. 61, pp. 239–248, Oct. 2021.
[15] S. Elaoud, R. Williamson, B. E. Sanli, and D. Xenos, "Multi-objective parallel batch scheduling in wafer fabs with job timelink constraints," in *Proc. Winter Simul. Conf. (WSC)*, London, U.K., Dec. 2021, pp. 1–11.
[16] M. C. May, S. Maucher, A. Holzer, A. Kuhnle, and G. Lanza, "Data analytics for time constraint adherence prediction in a semiconductor manufacturing use-case," *Proc. CIRP*, vol. 100, pp. 49–54, Jan. 2021.
[17] Y. Qiao, M. Zhou, N. Wu, Z. Li, and Q. Zhu, "Closing-down optimization for single-arm cluster tools subject to wafer residency time constraints," *IEEE Trans. Syst., Man, Cybern. Syst.*, vol. 51, no. 11, pp. 6792–6807, Nov. 2021.
[18] F. Yang, Y. Qiao, K. Gao, N. Wu, Y. Zhu, I. W. Simon, and R. Song, "Efficient approach to scheduling of transient processes for time-constrained single-arm cluster tools with parallel chambers," *IEEE Trans. Syst., Man, Cybern. Syst.*, vol. 50, no. 10, pp. 3646–3657, Oct. 2020.
[19] Y. Qiao, Y. Lu, J. Li, S. Zhang, N. Wu, and B. Liu, "An efficient binary integer programming model for residency time-constrained cluster tools with chamber cleaning requirements," *IEEE Trans. Autom. Sci. Eng.*, vol. 19, no. 3, pp. 1757–1771, Jul. 2022.
[20] Y. Lim, T.-S. Yu, and T.-E. Lee, "Adaptive scheduling of cluster tools with wafer delay constraints and process time variation," *IEEE Trans. Autom. Sci. Eng.*, vol. 17, no. 1, pp. 375–388, Jan. 2020.
[21] Y. Qiao, S. Zhang, N. Wu, M. Zhou, Z. Li, and T. Qu, "Efficient approach to failure response of process module in dual-arm cluster tools with wafer residency time constraints," *IEEE Trans. Syst., Man, Cybern. Syst.*, vol. 51, no. 3, pp. 1612–1629, Mar. 2021.
[22] J. Wang, H. Hu, C. Pan, Y. Zhou, and L. Li, "Scheduling dual-arm cluster tools with multiple wafer types and residency time constraints," *IEEE/CAA J. Automa. Sinica*, vol. 7, no. 3, pp. 776–789, May 2020.
[23] F. Yang, N. Wu, Y. Qiao, M. Zhou, R. Su, and T. Qu, "Modeling and optimal cyclic scheduling of time-constrained single-robot-arm cluster tools via Petri nets and linear programming," *IEEE Trans. Syst., Man, Cybern. Syst.*, vol. 50, no. 3, pp. 871–883, Mar. 2020.
[24] C. Pan and W. Xiong, "Analysis and optimizing of time delay for single-arm cluster tools under steady schedule," *Control Theory Appl.*, vol. 36, no. 10, pp. 1719–1729, 2019.
[25] D. Ru and D. Yu, "Topology optimization of end-effector of wafer transfer robot," *Agricult. Equip. Vehicle Eng.*, vol. 59, no. 4, pp. 84–88, 2021.
[26] M. Cong, X. Yu, B. Shen, and J. Liu, "Research on a novel R-$\theta$ wafer-handling robot," in *Proc. IEEE Int. Conf. Autom. Logistics*, Jinan, China, Aug. 2007, pp. 597–602.
[27] T. Li, F. Liu, Z. Li, M. Lu, and Q. He, "Analysis and experimental investigation of vibration characteristics of rotary platform of hydraulic excavator under complex working conditions," *Shock Vibrat.*, vol. 2021, pp. 1–10, Dec. 2021.
[28] J. Wang, C. Pan, H. Hu, L. Li, and Y. Zhou, "A cyclic scheduling approach to single-arm cluster tools with multiple wafer types and residency time constraints," *IEEE Trans. Autom. Sci. Eng.*, vol. 16, no. 3, pp. 1373–1386, Jul. 2019.
[29] Y. Qiao, N. Q. Wu, and M. C. Zhou, "Petri net modeling and wafer sojourn time analysis of single-arm cluster tools with residency time constraints and activity time variation," *IEEE Trans. Semicond. Manuf.*, vol. 25, no. 3, pp. 432–446, Aug. 2012.

**TINGHAO LI** was born in Guangzhou, China, in 1998. He received the B.S. degree in mechanical design manufacture and automation from Guangxi University, Nanning, China, in 2020. He is currently pursuing the M.S. degree in intelligent technology with the Institute of Systems Engineering, Macau University of Science and Technology (MUST), Macau, China. His research interests include intelligent manufacturing, scheduling, and control.

**ZHANGUANG ZHENG** received the M.S. and Ph.D. degrees in mechanical engineering from Guangxi University, Nanning, China, in 2004 and 2010, respectively. He is currently a Professor and a Ph.D. Supervisor at Guangxi University. His research interests include intelligent manufacturing, digital twins, and fatigue damage.